

RESEARCH ARTICLE | MAY 07 2024

Theoretical investigations on the natural bond orbital, HOMO-LUMO, contour maps, and energy gap of diatrizoate




Huda M. Jawad ✉; Farah A. Jasim




AIP Conf. Proc. 3097, 090004 (2024)

<https://doi.org/10.1063/5.0209811>






Lock-in Amplifier



Boxcar Averager

Boost Your Optics and Photonics Measurements

 Zurich Instruments

[Find out more](#)

Theoretical Investigations on the Natural Bond Orbital, HOMO-LUMO, Contour Maps, and Energy Gap of Diatrizoate

Huda M. Jawad^{1, a)} and Farah A. Jasim^{1, b)}

¹*Department of Physics, College of Science, Mustansiriyah University, Baghdad, Iraq*

^{a)} *Corresponding author: Farah.A.J@uomustansiriyah.edu.iq*

^{b)} *drhuda222@uomustansiriyah.edu.iq*

Abstract. In diagnostic radiography, a substance known as amidotrizoate—more often known by its previous name, diatrizoate—is an iodinated radiopaque X-ray contrast medium. When doing X-ray imaging, a contrast agent is used. Given that X-rays are unable to pass through the iodine moiety of diatrizoate, this compound blocks the film from being exposed to radiation. On an X-ray film, this makes it possible to view the various structures of the body and differentiate between bodily parts that contain and do not contain diatrizoate meglumine. Throughout the entirety of the Gaussian 09 program, each calculation was performed using the density functional theory with the use of the 6-31G basis set B3LYP as the level. Throughout the course of the geometry optimization, the geometrical structure, natural bond orbital, HOMO-LUMO, surfaces, contour maps and energy gap were developed. The results of the geometric optimization of diatrizoate demonstrated that natural bond orbital is an effective technique for researching the distribution of Mulliken charges. The electrostatic potential of the surface was determined to be the electron donor–acceptor. Increasing polarization in the carbonyl function groups leads to electrons transferring to excitation levels. The fluorescence process occurred when X-rays fell on these functional groups with fluorescence found, thus providing more resolution to the medical images used for medical diagnosis of any part of the body photographed with X-rays.

INTRODUCTION

Technical limitations slowly lead to the development of radiocontrast agents. X-ray photography, fluoroscopy and other medical imaging technologies, such as computed tomography (CT) and ultrasound, intensify the vascular structures and organs' visibility [1]. The benzene ring is the main structure, and the iodinated contrasts consist of atoms 1, 3, and 5 in the benzene ring. As for the diatrizoate substituent, the iodine atoms symmetrically take the second, fourth, and sixth positions in this ring [2], as shown in Figure (1).

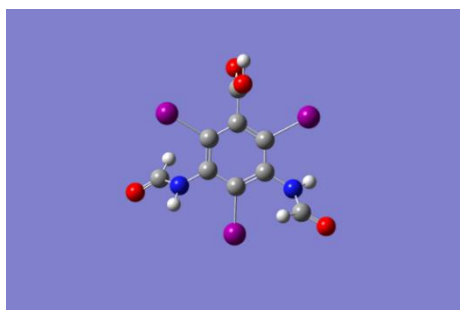


FIGURE 1. Diatrizote structure

Hoppe created the first diatrizoate contrast agent in 1956 by adding the acetylamino group to the triiodobenzene ring [3]. Given that iodine is an ionic agent that works to produce positive and negative ions when soluble in water, it

helps reduce toxicity. Animal studies have shown that (1, 3, and 5 diatrizoate) it is a fundamental radical molecule with OH substituents. The benzene ring forms a link with three OH atoms, thus increasing the molecule's solubility. Ionic and non-ionic contrast agents based on iodine are the two standard classifications [4]. A theoretical study of the diatrizoate structure to be analyzed by natural bond orbital (NBO), HOMO LUMO, and electrostatic surface, there are many studies that study these properties of many materials, including. Maged H. et al. study geometry optimization infrared spectra and some electronica properties have been achieved [5]. M. Kavimani et al. [6] presented theoretical and experimental investigations the vibrations and structure of naphthalen-2-lyoxy-acetic acid (NLA). Mina H. [7] used density functional theory (DFT) to improve the geometry of 1,2,7-thiadiazepane and analyzed the NBO based on the B3LYP/cc-pVDZ geometry to study the stereo electronic properties on the constancy of stereoisomers (equatorial-equatorial, axial-equatorial, and axial-axial). The results led them to the conclusion that the most stable stereoisomers are axial-axial or axial-equatorial.

Li X. et al. [8] introduced a theoretical study of the population analysis for NBO of compounds (para-substituted O-nitrosyl carboxylate) by using DFT (B3LYP) at the 6-31G (d, p) basis set. Their results emphasized the sigma bond's weakness in the O3-N2. Additionally, the inclusion of partial groups and the Hammett constants for the substituent resulted in a decrease in the charge transfer energy, and the vacancy of the contained $\sigma_{O_3-N_2}^*$ orbital is reduces in the perfect Lewis structure or increases $\sigma_{O_3-N_2}^*$ in the non-Lewis orbital. As a result, the distribution of charges on the structural atoms may match expectations. E. Hapeshi et al. [9] presented a theoretical study of iodinated X-ray iohexol and diatrizoate in the microbial degradation of municipal wastewater and revealed the presence of a bacterial consortium in wastewater, including several Nitrisporae, Firmicutes and Proteobacteria species. The best ICM elimination values were 79% for IOX and 73% for DTZ, and for each compound, 13 and 14 biotransformation products were found, respectively. Huda M. J. [10] investigated the electrical and spectral characteristics of hydroxychloroquine to knowledge more about its behavior and potential medicinal applications.

A. N. Isaev [11] designed hydrogen bonded C-H...Y (Y = O, S, Hal) Molecular theoretically. Their results showed that in the s-component in the NBO lone pair of the Y-acceptor, energy is raising at a larger proportion in complexes of methane and its halogen-substituted derivatives. Different measurements of CY distances demonstrated the complexes' equilibrium geometry in the area where the energy of E (2) was changed stoichiometrically and higher in the length C-H covalent bond that the distance was various R (CY).

This research focuses on studying the electronic excitation energy of diatrizoate and investigating the energetic behavior and interactions associated with the structural properties of diatrizoate computationally depending on DFT.

The control of intermolecular orbital interaction in the molecule was investigated using orbital energy based on NBOs to explore the charge transfer from loaded contributor NBOs to unoccupied acceptor NBOs. This information was then used to determine the rule. To determine the relative importance of the energy that each donor and receiver contribute to NBO, second-order perturbation theory is applied. The fundamental aspects of quantum chemistry, known as HOMO-LUMO and the energy gap, demonstrate the chemical reactivity and dynamic constancy of molecules. The HOMO-orbital predominantly performances as an electron contributor, whereas the LUMO-orbital predominantly performances as an electron acceptor [12].

COMPUTATIONAL METHODS

The Gaussian 09 software package was utilized for all computations and three-dimensional analyses. The standard density functional theory 6-31G (d, p) basis set function [13] was used to explain the mathematical calculations of systems that contain C, H, N, I and O. Becker's hybrid three-parameter exchange functional and Lee, Yang and Parr's (B3LYP) nonlocal correlation functional were used for the optimization of the diatrizoate shape [14]. In addition, the natural bond orbital method was utilized in the process of carrying out population analysis [15]. The bonding orbital that was computed and found to have the highest electron density was referred to as NBO. Afterwards, frequency mathematical calculations were used to validate the minimum state of the consequence geometries. Then, NBO was investigated using the NBO Gaussian software [16]. Non-orthogonal atomic orbitals (AOs) were used as a starting point for the creation of sets of natural AOs (NAOs), natural hybrid orbitals (NHOs) and natural binary orbitals (NBOs). Taking into account that electron density along with additional properties are defined by the fewest occupied orbitals with the quickest convergence, these localized basis sets are complete and could appropriately describe the wave functions. The filled NBOs were utilized in the process of describing the hypothetical Lewis structure that was strictly localized. Calculating delocalization, a measure of how much the particle deviates from the Lewis configuration, is possible by using the dealings between the filling and anti-bonding (Rydberg) orbitals. Quantitatively analyzing the noncovalent bonding-antibonding interaction is possible using the NBO technique [17].

This study aimed to investigate the base set dependence of the DFT HOMO and LUMO energies. Recording the vibrational frequency of diatrizoate allowed for the creation of vibrational analysis that was based on the same premise. The empty molecular orbital energy is at its lowest and the occupied molecular orbital energy is at its highest in molecules (EHOMO) (ELUMO). Certain mathematical calculations were carried out concerning the electrostatic surface of diatrizoate.

RESULT AND DISCUSSION

Charges of Mulliken Atomic

The computation of charges of Mulliken atomic is necessary in the presentation of quantum chemical mathematical calculations to molecule arrangements because atomic charges have an effect happening the electronic structure, molecular polarisability, dipole moment and various other characteristics of molecular systems [18, 19]. Atomic charge has been applied to the problem of elucidating the mechanisms underlying charge transfer and the equalization of electronegativity that occurs in the course of chemical reactions. The charge placed on the atoms in their arranged configuration showed that the formation of donor and acceptor pairs is an essential stage in the process of charge transfer within the molecule [20].

TABLE 1. Charges of Mulliken atomic calculated by B3LYP/ 6-31G (d, p) method only

Atom	Charge	Atom	Charge
C ₁	-0.408411	C ₂	0.237779
C ₃	-0.431463	C ₆	0.229824
C ₄	-0.000067	C ₇	0.61755
N ₁₁	-0.64151	I ₈	0.346753
O ₁₅	-0.386726	I ₉	0.380509
O ₁₆	-0.445523	I ₁₀	0.366819
O ₁₇	-0.558385	H ₁₂	0.324113
N ₁₉	-0.63498	C ₁₃	0.336044
O ₂₃	-0.38555	H ₁₅	0.205476
.....	H ₁₈	0.384731
.....	H ₂₀	0.32308
.....	C ₂₁	0.337708
.....	H ₂₂	0.20283

Table 1 shows (C₂, C₆, C₇, I₈, I₉, I₁₀, H₁₂, C₁₃, H₁₅, H₁₈, H₂₀, C₂₁ and H₂₂) with a positive charge and (C₁, C₃, C₄, N₁₁, O₁₅, O₁₆, N₁₉ and O₂₃) with a negative charge [21]. Nitrogen (N₁₁, N₁₉) has a maximum negative charge value of about -0.64151 and -0.63498 in the C-N functional group; O₁₇ in the OH group; and O₁₅, O₁₆ and O₂₃ in the CH functional group. Carbonyls are determined by the polarization of the C=O bond but the atoms that are next to the bond also have a role in determining its specific reaction pathways [22]. C₇ has a maximum positive charge value of around 0.61755.

Natural Bond Orbital

Analysing charge transfer or conjugative interactions is possible using NBO analysis, in addition to bonding, intramolecular and intermolecular interactions and interactions between ligands in a molecular system [23]. A sustained donor-acceptor interaction is the result of electron density delocalisation between occupied Lewis-type NBO orbitals (lone pair or and bonding) and empty (anti-bonding or Rydberg) non-Lewis NBO orbitals. This delocalization occurs between Lewis-type NBO orbitals that are not Rydberg orbitals. By using on-molecule NBO analysis, an enhanced understanding of intermolecular hybridisation and intermolecular electron density could be gained. According to Panja S. et al. [24], the process of intermolecular charge transfer (ICT) in acceptor-donor systems is very important in various physical and biological systems.

The orbital intersection of the (C-C) and (C-C) bond orbits causes the ICT to stabilise the system. The electronic density is increased by C-C interactions. The diatrizoate in this work has 244 electrons. Few selected orbitals were displayed and the remainder were only mentioned. The formula for 0.7058 C (SP^{1.56}) + 0.7084C is roughly (SP^{1.74}).

The weights were calculated using the squares of the coefficients and they have the value $(0.7058)^2 = 0.4882$, which indicates a localisation of 48.82% on carbon C₁. The 50.18% localisation on carbon C₂ was obtained in a similar manner. The SP^{1.56} hybrid on carbon, which is a combination of (49.82%) s and (50.18%) p, produced the (C₁-C₂) bond. Meanwhile, the P100 on carbon [which is a mixture of (50.79%) P, (49.21%) P] and P 99.99 on carbon [which is a mixture of C₁ (50.7% 1) P, C₂ (49.29%) P] was used to generate p bonds in C₁-C₂ and C₅-C₆, which equate to a pi bond carbon. O₁₇-H₁₈ and N₁₉-H₂₀ bonds were created from sp^{4.41} hybrids on oxygen and transitioned to pure S100 orbitals and the N₁₉-H₂₀ bonds were created from SP^{2.58} hybrids on nitrogen and transitioned to pure S100 orbitals because the hydrogen atom has a high electronegativity, which attracts electrons to it [25]. This label specifies the type 'CR' for a one-centre core pair for each NBO (30–113). The 'LP' for one-centre valence lone pair for each NBO (114–132) stands for the respective lone pairs on oxygen (O₂) and nitrogen (N). 'RY*' stands for one-centre Rydberg for each NBO (133–215). The unstarred and starred designations for each NBO (216–244) 'BD*' for two-centre anti-bonding correspond to Lewis and non-Lewis NBOs, respectively. The weakening has been attributed to this accumulation of density in the latter anti-bond [26].

TABLE 2. Polarization coefficient, hybrid and atomic orbital contribution in selected natural bond orbital for diatrizoate

Bond orbital	Hybrid (a)	Atomic orbital (%)	Polarization coefficient	Hybrid (b)	Atomic orbital (%)	Polarization coefficient
σ C ₁ -C ₂	SP ^{1.56}	49.82	0.7058	SP ^{1.74}	50.18	0.7084
π C ₁ -C ₂	P ^{99.99}	50.71	0.7121	P ^{99.99}	49.29	0.7021
σ C ₁ -C ₆	SP ^{1.57}	49.88	0.7063	SP ^{1.76}	50.21	0.7080
σ C ₁ -I ₈	SP ^{3.55}	57.26	0.7567	SP ^{3.17}	42.74	0.6538
σ C ₂ -C ₃	SP ^{1.76}	50.21	0.7080	SP ^{1.57}	49.88	0.7062
σ C ₂ -N ₁₁	SP ^{2.68}	39.70	0.6301	SP ^{1.81}	60.30	0.7765
σ C ₃ -C ₄	P ^{1.56}	49.26	0.7019	P ^{1.83}	50.74	0.7123
σ C ₃ -I ₁₀	SP ^{3.54}	57.03	0.7552	SP ^{3.13}	42.97	0.6555
σ C ₄ -C ₅	SP ^{1.84}	50.79	0.7126	SP ^{1.58}	49.21	0.7015
σ C ₄ -C ₇	SP ^{2.3.9}	53.37	0.7306	SP ^{1.56}	46.63	0.6828
π C ₅ -C ₆	P ¹⁰⁰	50.46	0.7104	P ¹⁰⁰	49.54	0.7038
σ C ₅ -I ₉	SP ^{3.4}	57.43	0.7578	SP ^{3.0}	42.57	0.6525
σ C ₆ -N ₁₉	SP ^{2.69}	39.68	0.6300	SP ^{1.80}	60.32	0.7766
σ C ₇ -O ₁₆	SP ^{2.03}	34.10	0.5839	SP ^{1.54}	65.90	0.8118
σ N ₁₁ -C ₁₃	SP ^{1.76}	64.89	0.8055	SP ^{2.28}	35.11	0.5926
σ C ₁₃ -H ₁₄	SP ^{1.72}	60.05	0.7749	S ¹⁰⁰	39.95	0.6320
σ C ₁₃ -O ₁₅	SP ^{5.49}	35.02	0.5917	SP ^{4.88}	64.98	0.8051
σ C ₁₇ -H ₁₈	SP ^{4.41}	73.94	0.8599	S ¹⁰⁰	29.06	0.5105
σ N ₁₉ -H ₂₀	SP ^{2.58}	72.20	0.8497	S ¹⁰⁰	27.80	0.5273
σ N ₁₉ -C ₂₁	SP ^{1.76}	64.91	0.8057	SP ^{2.29}	35.09	0.5924

Table 3 shows donor (I) and acceptor (J) with transition second order energy E^2 and energy gap ($E_i - E_j$) and F is the standard deviation. Values higher than 8 Kcal/mol and smaller than 8 are usually for σ bond. All the lines with CR (core) and Ry* (Rydberg) were ignored except the transition from (BD or LP) bonding orbital or lone pair (LP) electrons to anti-bonding orbital (BD*) or (BD*) to (BD) in case of back donation. The perturbation energies of acceptor-donor interactions are shown in the title diatrizoate molecule, π (C₁-C₂) to π^* (C₃-C₄) has 18.08 kJ/mol and π (C₁-C₂) to π^* (C₅-C₆) has 19.11 kJ/mol. The C-C bond's anti-C-C bond in the benzene ring stabilised because of the interaction of the σ and the π electrons intramolecular hyperconjugation in the ring due to resonance within the ring [27].

In π (O₁₇) to π^* (C₇-O₁₆), 1.99965 is the maximum occupancy Lone pairs that interact with the anti-bonding C₇-O₁₆ orbital when O is in this conformation, depending on how they are positioned in relation to the C₇-O₁₆ bonds [28]. Maximum occupancies of 1.98172 were obtained for the σ bond iodine I₁₀. The same type of interaction, which is linked to the molecule's resonance, involves electron donation from LP (1) I₁₀ to σ^* (C₅-C₆), which exhibited little stabilisation (10.69 kJ/mol), and from LP (2) O₁₅ to (N₁₁-C₁₃), which exhibited significant stabilisation energies (30.98

kJ/mol). Meanwhile, O_{23} to π^* (N_1 - C_2) and LP (2) O_{16} to (C_7 - O_{17}) led to the highest stabilisation energies. A strong orbital interaction was found between π^* (C_7 - O_{16}) to π^* (N_{19} - C_{21}).

TABLE 3. Polarization coefficient, hybrid and atomic orbital contribution in selected natural bond orbital for diatrizoate

Donor (i)	Type	Occupancy	Acceptor (j)	Type	Occupancy	E ² [Kcal/ mol]	Ej- Ei [a.u.]	F(I,j) [a.u.]
C ₁ -C ₂	π	1.68205	C ₃ -C ₄	π^*	0.39292	18.08	28.0	0.065
C ₁ -C ₂	π	1.68205	C ₅ -C ₆	π^*	0.41286	19.11	0.27	0.066
C ₃ -C ₄	π	1.68142	C ₁ -C ₂	π^*	0.03182	19.84	0.27	0.067
C ₃ -C ₄	π	1.68142	C ₅ -C ₆	π^*	0.41286	19.10	0.27	0.066
C ₅ -C ₆	π	1.67380	C ₁ -C ₂	π^*	0.03182	19.04	0.27	0.065
C ₅ -C ₆	π	1.67380	C ₃ -C ₄	π^*	0.39292	20.25	0.28	0.069
O ₁₇	π	1.99965	C ₇ -O ₁₆	π^*	0.03195	53.16	0.29	0.112
C ₁ -C ₂	π	1.68205	C ₃ -C ₄	π^*	0.39292	18.08	0.28	0.079
C ₅ -C ₆	π	1.67380	C ₃ -C ₄	π^*	0.39292	18.08	0.28	0.081
C ₃ -C ₄	π	1.68142	C ₇ -O ₁₆	π^*	0.23855	16.74	0.27	0.061
I ₁₀	LP (1)	1.99679	C ₅ -C ₆	π^*	0.41286	10.69	0.24	0.048
O ₁₅	LP (2)	1.83611	N ₁₁ -C ₁₃	σ^*	0.09415	30.98	0.62	0.136
O ₁₅	LP (2)	1.83611	C ₁₃ -H ₁₄	σ^*	0.06087	19.30	0.62	0.103
O ₁₆	LP (2)	1.80247	C ₄ -C ₇	σ^*	0.07982	20.93	0.62	0.105
O ₁₆	LP (2)	1.80247	C ₇ -O ₁₇	σ^*	0.12809	39.90	0.53	0.132
O ₁₇	LP (2)	1.78332	C ₇ -O ₁₆	σ^*	0.03195	53.16	0.29	0.112
C ₇ -O ₁₆	π^*	0.03195	C ₃ -C ₄	π^*	0.39292	52.76	0.03	0.064
O ₂₃	LP (2)	1.83630	N ₁₉ -C ₂₁	σ^*	0.09456	31.06	0.62	0.126

TABLE 4. Diatrizoate directionality and ‘bond bending’ (deviations from the line of nuclear centers)

Bond Orbital	Deviation Angle (degree)		Line of Centers	
NBO	Deviation Hybrid (a)	Deviation Hybrid (b)	Polar θ	Azimuthal ϕ
C ₁ -C ₂	1.0	3.0	90	223.1
C ₂ -N ₁₁	1.3	1.2	90	164.7
C ₆ -N ₁₉	3.1	1.2	87	44.6
C ₇ -O ₁₇	7	2.2	27.6	254.4
N ₁₁ -H ₁₂	4.4	-----	141.4	204.5
C ₁₃ -H ₁₄	6.6	----	39.9	12.5
N ₁₉ -H ₂₀	3.2	-----	40.5	91.0
C ₂₁ -H ₂₂	6.6	-----	139.7	258.9
C ₂₁ -O ₂₃	7.3	-----	87.9	46.2

The polar (theta) and azimuthal (phi) angles were used to characterize the orientation of a hybrid's p-component vector (in the ESS coordinate system). The hybrid orientation has been contrasted to the orientation of the line of centres connecting the two nuclei to limit the bond's bending or deviation angle. A carbon of the sigma C-C bond (NBO 1) in the diatrizoate state illustrated in Table (4) is 3.0 degrees curved but almost parallel to the C-C axis, away from the line of C-C centres (within the 1.0-degree criterion). The sigma C₂-N₁₁ bond (NBO6) was twisted away from the C-N line by 1.3 degrees, whereas the nitrogen was generally aligned with the C-N axis (at the 1.2-degree threshold). For the sigma C-N bond (NBO15), where the nitrogen was roughly bound to the C-N axis at 1.2-degree threshold, the carbon was twisted away from the C-N axis by 1.3 degrees.

Meanwhile, the carbon in the sigma C-O bond (NBO18) was twisted away from the line of C-O by 3.1 degrees and the oxygen was roughly aligned with the C-O axis (within the 1.2-degree threshold). The nitrogen's sigma N-H bond (NBO19) was bent 4.4 degrees away from the N-H line. The carbon atoms in the sigma C-H bond (NBO21)

were 6.6 degrees bent away from the C-H and N-H lines. The nitrogen of the sigma N-H bond (NBO25) bent away from the line of N-H by 3.2 degrees. This information is very helpful in forecasting the direction of geometry-related events.

Electrostatic Potential Surface

Figure 2 presents a mapping of the electrostatic potential (ESP) and electron density (ED) of diatrizoate. In ESP, the negative potential is centred in the region immediately surrounding the oxygen atoms, whereas the positive potential is centred on the surface of the remainder. It has been a common concept in the chemical literature and it is typically utilised to indicate locations that are abundant in electrons [29-31].

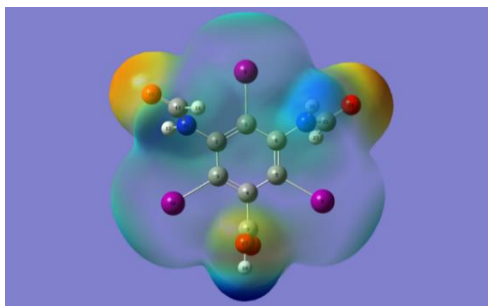


FIGURE 2. The electrostatic potential surface of diatrizoate

The electric charge that is carried by the molecule MESP is the glue that holds together the disparate concepts of chemical reactivity site, electronegativity, partial charges and total charge distribution. It offers a graphical depiction of the relative polarity of a molecule. It could also be utilised to explain hydrogen bonding, reactivity and the structure–activity relationship of various compounds, such as biomolecules and medications. It is the potential energy that a proton possesses when it is at a certain position in close proximity to a molecule. ESP is still a reliable predictor of whether a molecule could react favourably or unfavourably with positively or negatively charged reactants. A correlation exists between the colours that appear on the surface of a molecule and the electrical potentials that they represent. Locations that have the potential to entice people are typically denoted by red, whilst places that are more likely to turn people away are typically denoted by blue.

The attraction of the proton to the highly concentrated electrons in the molecules is the source of the electron cloud's negative electric potential (from lone pairs, pi-bonds). A positive electrostatic potential is created in locations with low electron concentrations due to the partial shielding of the nuclear charge and the attraction of the proton to the atomic nuclei. The atom with the same name contains positive potentials close to the hydrogen and nitrogen atoms, whereas the atom with the same name contains negative potentials close to the oxygen atom.

Contour Maps

The contours of ED were used to characterize the electrostatic potential's forms. On occasion, contour maps could be expressed using Brillion zones. Sometimes it is possible to argue that the system's electrostatic potential is described by its contours. It looks for active locations inside the paradigm's geometry.

Some researchers described how ED is distributed in space by using the term contour and explained how the geometrical system's dispersion is mapped out in the interaction. Atom, which leads to the foretelling that charge transfer could occur, leads to the prediction that contour schematics could gain new geometrical properties across contour geometry [5]. Charge diffusion was found in the structure of diatrizoate on the right and left side, that is to say, this variation in charge diffusion is produced because of the interaction between oxygen atoms with carbon and hydrogen atoms. The contour maps are illustrated in Figure 3.

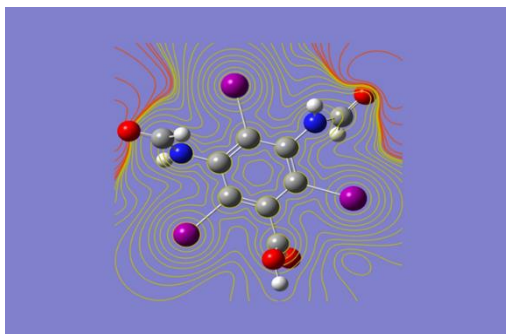


FIGURE 3. Contours map for diatrizoate

HOMO-LUMO

Figure 4 demonstrates that the HOMO energy has a relatively high value. Lower values of LUMO energy indicate an increased possibility of receiving electrons and they describe a molecule's propensity to donate electrons to the appropriate acceptor molecule when it has a low empty molecular orbital energy [32].

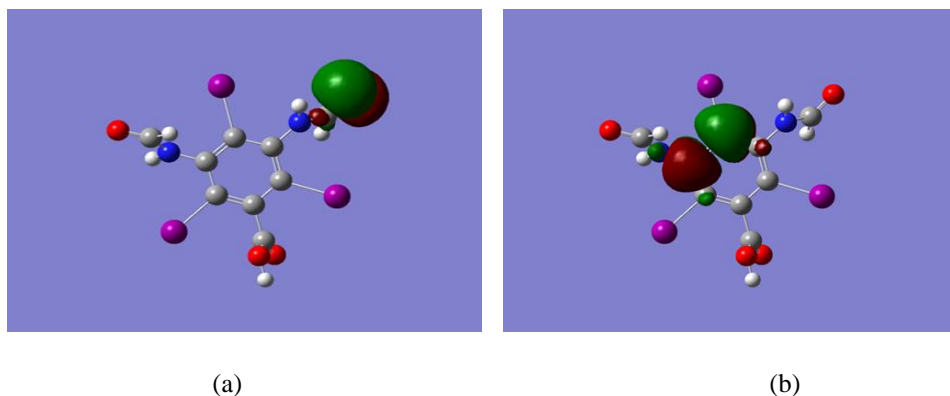


FIGURE 4. (a) HOMO, (b) LUMO plot of diatrizoate

In other words, lower values of LUMO energy indicate a greater possibility of receiving electrons. The image evidently showed how the charge density in the isolated molecule is shifting from one part of the molecule to the other, thereby producing an energy gap equal to ELUMO minus EHOMO [33]. In terms of HOMO, the majority of the charge that is accumulated comes from the C1=C2 section. In the LUMO state, the charge was obtained using the equation $C21=O23$ and the energy gap remained the same (0.4.37 eV).

CONCLUSION

Some theoretical research was carried out to optimise the geometry of diatrizoate. The DFT method was applied while computing the molecular structure's overall geometry. NBO analysis was used to determine the degree to which the hyper-conjugative interaction and charge delocalisation contribute to the stability of the molecule. The nature of the charge transfer taking inside the molecule was determined by employing HOMO and LUMO studies.

The DFT approach was also utilised to finish MEP. The results showed that the donor and acceptor are most likely to be located in the ring atoms and the substitution atoms. It is essential for the molecule's stability that the C-C, C-H, C-O, N-H, H-O and I-C interactions, which make up the majority of intermolecular interactions, exist between the atoms. The ICT that is produced as a result of the orbital overlap that occurs between the (C-C) and (C-C) bond orbits in the compound diatrizoate helps keep the system in a stable state. Interactions between carbon atoms or C-C interactions could lead to a rise in ED. When X-rays hit these functional groups with fluorescence already present, the fluorescence process begins, thus raising the level of polarization in the carbonyl function groups and making it

possible for electrons to transfer to higher excitation levels. This phenomenon results in an increase in the resolution of medical images for the purpose of improving the accuracy of medical diagnosis of any portion of the body that is scanned using X-rays.

ACKNOWLEDGMENTS

The authors would like to express their gratitude to Mustansiriyah University (www.uomustansiriyah.edu.iq) in Baghdad, Iraq, for its assistance with this work.

REFERENCES

1. J. Safura, S. Khazaei, H. Behnammanesh, M. Laranjo, D. Beiki, and M. Filomena Botelho. "X-ray-based cancer diagnosis and treatment methods," in *Electromagnetic Waves-Based Cancer Diagnosis and Therapy*, pp. 239-294. Academic Press, (2023).
2. B. Yuki, M. Jekel, and A. Putschew. "Can reductive deiodination improve the sorption of iodinated X-ray contrast media to aquifer material during bank filtration?," *Chemosphere* 326 (2023): 138438.
3. F. ALDIBASHI, S. KANDEMIRLI, and F. KANDEMIRLI. "Molecular structure and electronic properties of diatrizoate, ioxaglate contrast compounds by quantum chemical calculations," *Erciyes Üniversitesi Fen Bilimleri Enstitüsü Fen Bilimleri Dergisi* 36, no. 2 (2020): 204-213.
4. G. S. Hitinder. "Renal Complications in the Catheterization Laboratory," *An Issue of Interventional Cardiology Clinics*. Vol. 3, no. 3. Elsevier Health Sciences, (2014).
5. H. M. Maged, A. S. Alwan, and M. L. Jabbar. "Electronical Properties for (C_xH_yZ₂-NO) Nanoclusters," *Current Nanomaterials* 2, no. 1 (2017): 33-38.
6. M. Kavimani, V. Balachandran, B. Narayana, and K. Vanasundari. "Conformational stability, spectroscopic (FT-IR, FT-Raman) analysis, fukui function, Hirshfeld surface and docking analysis of Naphthalene-2-lyoxy acetic acid by density functional theory," (2017).
7. M. Haghdadi. "DFT molecular orbital calculations and natural bond orbital analysis of 1, 2, 7-thiadiazepane conformers," *Monatshefte für Chemie-Chemical Monthly* 144 (2013): 1653-1661.
8. L. Xiao-Hong, C. Qing-Dong, and Z. Xian-Zhou. "Natural bond orbital population analysis of para-substituted O-nitrosyl carboxylate compounds," *Structural Chemistry* 20, no. 6 (2009): 1043.
9. E. Hapeshi, A. Lambrianides, P. Koutsoftas, E. Kastanos, C. Michael, and Despo Fatta-Kassinou. "Investigating the fate of iodinated X-ray contrast media iohexol and diatrizoate during microbial degradation in an MBBR system treating urban wastewater," *Environmental Science and Pollution Research* 20 (2013): 3592-3606.
10. H. M. Jawad. "Study of the Electronic and Spectrum Properties for a Medication Hydroxychloroquine," in *Journal of Physics: Conference Series*, vol. 2322, no. 1, p. 012065. IOP Publishing, 2022.
11. A. N. Isaev. "Hydrogen bonded C-H... Y (Y= O, S, Hal) molecular complexes: A natural bond orbital analysis," *Russian Journal of Physical Chemistry A*, 90, 601-609, (2016).
12. M. Karabacak, A. M. Asiri, A. O. Al-Youbi, A. H. Qusti, and M. Cinar. "Identification of structural and spectral features of synthesized cyano-stilbene dye derivatives: A comparative experimental and DFT study," *Spectrochimica Acta Part A: Molecular and Biomolecular Spectroscopy* 120 (2014): 144-150.
13. R. Jindal, V. Sharma, and A. Shukla. "Density functional theory study of the hydrogen evolution reaction in haeckelite boron nitride quantum dots," *International Journal of Hydrogen Energy* 47, no. 99 (2022): 41783-41794.
14. A. D. Beeke. "Density-functional thermochemistry. III. The role of exact exchange," *J. Chem. Phys.*, 98(7), 5648-6, (1993).
15. A. E. Reed, L. A. Curtiss, and F. Weinhold. "Intermolecular interactions from a natural bond orbital, donor-acceptor viewpoint," *Chemical Reviews*, 88(6), 899-926, (1988).
16. N. K. Nkungli, J. N. Ghogomu, L. N. Nogheu, and S. R. Gadre. "DFT and TD-DFT study of Bis [2-(5-Amino-[1, 3, 4]-oxadiazol-2-yl) Phenol](Diaqua) M (II) complexes [M= Cu, Ni and Zn]: electronic structures, properties and analyses," *Computational Chemistry*, 3(03), 29, (2015).
17. M. Haghdadi. "DFT molecular orbital calculations and natural bond orbital analysis of 1, 2, 7-thiadiazepane conformers," *Monatshefte für Chemie-Chemical Monthly*, 144, 1653-1661, (2013).

18. S. Bharanidharan, S. Savithiri, G. Rajarajan, P. Sugumar, and A. Nelson. "Synthesis, spectroscopic profiling, biological evaluation, DFT, molecular docking and mathematical studies of 3, 5-diethyl-2r, 6c-diphenylpiperidin-4-one picrate," *Molecular Physics*, 121(4), e2173964, (2023).
19. G. Ramesh, and B. V. Reddy. "Investigation of Barrier Potential, Structure (Monomer & Dimer), Chemical Reactivity, NLO, MEP, and NPA Analysis of Pyrrole-2-Carboxaldehyde Using Quantum Chemical Calculations," *Polycyclic Aromatic Compounds*, 1-15, (2022).
20. L. Hansol, D. Lee, D. Hun Sin, S. Woo Kim, M. Seok Jeong, and K. Cho. "Effect of donor-acceptor molecular orientation on charge photogeneration in organic solar cells," *NPG Asia Materials* 10, no. 6 (2018): 469-481.
21. R. Gangadharan, and K. Sampath. "Natural Bond Orbital (NBO) population analysis of 1-azanaphthalene-8-ol," *Acta Physica Polonica A*, 125(1), 18-22, (2014).
22. D. E. Almonacid, E. R. Yera, J. B. Mitchell, and P. C. Babbitt. "Quantitative comparison of catalytic mechanisms and overall reactions in convergently evolved enzymes: implications for classification of enzyme function," *PLoS computational biology*, 6(3), e1000700, (2010).
23. A. E. Reed, L. A. Curtiss, and F. Weinhold. "Intermolecular interactions from a natural bond orbital, donor-acceptor viewpoint," *Chemical Reviews*, 88(6), 899-926, (1988).
24. S. K. Panja, N. Dwivedi, S. Saha. "Tuning the intramolecular charge transfer (ICT) process in push-pull systems: effect of nitro groups," *RSC advances*, 6(107), 105786-105794, (2016).
25. M. Benedetti, F. De Castro, A. Ciccarese, and F. P. Fanizzi. "Is hydrogen electronegativity higher than Pauling's value? New clues from the ¹³C and ²⁹Si NMR chemical shifts of [CHF₃] and [SiHF₃] molecules," *Pure and Applied Chemistry*, 91(10), 1679-1686, (2019).
26. N. Salami, and A. Shokri. "Electronic structure of solids and molecules," *In Interface science and technology* (Vol. 32, pp. 325-373). Elsevier, (2021).
27. İ. Sıdır, G. S. Yadigar, K. Mustafa, and T. Erol. "Ab initio Hartree-Fock and density functional theory investigations on the conformational stability, molecular structure and vibrational spectra of 7-acetoxy-6-(2, 3-dibromopropyl)-4, 8-dimethylcoumarin molecule," *Journal of Molecular Structure* 964, no. 1-3 (2010): 134-151.
28. D. W. Szczepanik, M. Andrzejak, J. Dominikowska, B. Pawełek, T. M. Krygowski, H. Szatyłowicz, and M. Sola. "The electron density of delocalized bonds (EDDB) applied for quantifying aromaticity," *Physical Chemistry Chemical Physics*, 19(42), 28970-28981, (2017).
29. E. J. Braga, B. T. Corpe, M. M. Marinho, and E. S. Marinho. "Molecular electrostatic potential surface, HOMO-LUMO, and computational analysis of synthetic drug Rilpivirine," *Int. J. Sci. Eng. Res*, 7(7), 315-319, (2016).
30. B. Alankriti, H. S. Scott, T. Pham, K-J. Chen, B. Space, M. Lusi, M. L. Perry, and M. J. Zaworotko. "Towards an understanding of the propensity for crystalline hydrate formation by molecular compounds," *IUCrJ* 3, no. 6 (2016): 430-439.
31. M. Drissi, N. Benhalima, Y. Megrouss, R. Rachida, A. Chouaih, and F. Hamzaoui. "Theoretical and experimental electrostatic potential around the m-nitrophenol molecule," *Molecules*, 20(3), 4042-4054, (2015).
32. M. A. Abdulsattar, B. B. Kadhim, and H. M. Jawad. "Electronic, structural and vibrational properties of GaP diamondoids and nanocrystals: a density functional theory study," *Nanomaterials and Nanotechnology* 5 (2015): 15.
33. K. Barouni, A. Kassale, A. Albourine, O. Jbara, B. Hammouti, and L. Bazzi. "Amino acids as corrosion inhibitors for copper in nitric acid medium: Experimental and theoretical study," *J. Mater. Environ. Sci*, 5(2), 456-463, (2014).